

# A Semiparametric Nonlinear Mixed Effects Model with Penalized Splines Using Automatic Differentiation

Matteo D'Alessandro

Department of Biostatistics, University of Oslo  
and

Magne Thoresen

Department of Biostatistics, University of Oslo  
and

Øystein Sørensen

Department of Psychology, University of Oslo

March 13, 2026

## Abstract

We present an estimation procedure for nonlinear mixed-effects models in which the population trajectory is represented by penalized splines and adapted to individuals via subject-specific transformation parameters. By exploiting the mixed model representation of penalized splines, the level of smoothness can be estimated jointly with other variance components. The integration over random effects needed to obtain the marginal likelihood is carried out using the Laplace approximation. Exact derivatives for evaluation and maximization of the resulting likelihood are obtained via automatic differentiation implemented through Template Model Builder. In simulation studies, the method produces improved inferential performance and reduced computational burden when compared to the existing procedure. The approach is further illustrated through a case study on infant height growth in the first two years of life.

*Keywords:* automatic differentiation, Laplace approximation, longitudinal data, nonlinear mixed effects model, penalized splines.

# 1 Introduction

Longitudinal data, consisting of repeated measurements collected over time on the same experimental units, arise in many areas of research, including medicine, psychology, and the social sciences. Typical examples include growth or developmental trajectories, biomarker profiles such as serum glucose levels following a meal, or repeated assessments of behavioral or cognitive performance over time. Each unit yields a trajectory observed at a finite and possibly irregular set of time points. A common characteristic of such data is that the individual trajectories exhibit a similar underlying shape while differing in scale, timing, or other subject-specific features. Scientific interest often lies in studying both the population-level trajectory and the between-subject variability. By assuming a common trajectory, information can be pooled across subjects, improving estimation even when individual units are observed sparsely.

We consider the case where the population trajectory is estimated semi-parametrically, and adapted to each subject by a small set of individual transformation parameters expressed as random effects. This approach accommodates situations in which an explicit functional form of the population trajectory is not available, by representing it through spline expansions.

Different approaches have been proposed for this data problem. Self-modeling regression (SEMOR) was first introduced by [Lawton et al. \(1972\)](#) as,

$$f(\theta_i; x) = \theta_{0i} + \theta_{1i}g([x - \theta_{2i}]/\theta_{3i}) \tag{1}$$

with  $x$  denoting the independent variable and  $f(\theta_i; x)$  the individual-specific trajectory for subject  $i$ . The vector  $\theta_i = (\theta_{0i}, \theta_{1i}, \theta_{2i}, \theta_{3i})^\top$  contains subject-specific transformation parameters:  $\theta_{0i}$  and  $\theta_{1i}$  correspond to vertical shift and scale, while  $\theta_{2i}$  and  $\theta_{3i}$  control horizontal shift and scale. The function  $g$  was modeled as a first-order spline, and estimation of  $\theta_i$  and  $g$  was achieved via non-linear regression. [Lindstrom \(1995\)](#) extended the model by introducing

random effects on the transformation parameters and representing the common shape function via free-knot splines, reducing the number of total parameters. Estimation was achieved through approximate maximum likelihood using the Laplace approximations and the `nlme` algorithm (Lindstrom and Bates, 1990), and is now implemented in the package `sitar` (Cole et al., 2010). Other extensions of SEMOR include those of Coull and Staudenmayer (2004), who model multivariate curve data by introducing a latent function shared across curves from the same subject, and Altman and Villarreal (2004), who extended the model to allow the transformation parameters  $\theta$  in (1) to depend on time-invariant covariates.

Ke and Wang (2001) proposed a generalization of SEMOR that places it within a common framework for estimation and inference, alongside many other model classes. The resulting model, known as the semiparametric nonlinear mixed-effects model (SNMM), can be expressed in this form:

$$\begin{aligned}
 y_{ij} &= \eta(\phi_i, f; t_{ij}) + e_{ij}, \quad i = 1, \dots, m, \quad j = 1, \dots, n_i, \\
 \phi_i &= \mathbf{A}_i \beta + \mathbf{B}_i \mathbf{b}_i, \quad \mathbf{b}_i \sim N(\mathbf{0}, \sigma^2 \mathbf{G}),
 \end{aligned}
 \tag{2}$$

where  $y_{ij}$  represents the  $j$ th response for subject  $i$ , and  $t_{ij}$  is a covariate. The function  $\eta$  is known and depends on  $t_{ij}$ , the parameter vector  $\phi_i$  is of dimension  $r$ , and  $f$  is an unknown function. The vector  $\beta$  is a  $p$ -dimensional vector of fixed effects, while  $\mathbf{b}_i$  is a  $q$ -dimensional vector of random effects associated with subject  $i$ .  $\mathbf{A}_i$  and  $\mathbf{B}_i$  are design matrices associated with the fixed and random effects. The main advantage of the SNMM is its very general formulation which makes it flexible to various data settings and modeling assumptions. It can also be used to assess the adequacy of a particular functional form in a non-linear mixed model (Ke and Wang, 2001, Section 6). The complexity of the SNMM, however, introduces difficulties: the estimation of these types of models is usually done by “integrating out” the random effects from the full likelihood to obtain the marginal likelihood; in the case where the random effects enter the likelihood non-linearly, no closed form solutions exist, and

approximations are necessary. Moreover,  $f$ ,  $\beta$ , and  $\mathbf{b}$  may interact in ways that complicate estimation.

Ke and Wang (2001) model the population curve  $f$  with a smoothing spline. The *double-penalized marginal likelihood* (which includes a penalty related to smoothness and one to the subject random effects) is optimized iteratively by use of `nlme` and a routine for spline estimation. The method is implemented in the R package `assist` (Wang and Ke, 2004), and procedures for inference on both the parametric components and the nonparametric function are provided.

This approach has some limitations: (i) as noted by Elmi et al. (2011), the estimation algorithm separates the likelihood associated with the shape function from that associated with the fixed and random effects, which doesn't guarantee that the iterative procedure converges to a maximizer of the joint likelihood. Moreover, variance estimates obtained from separate likelihoods will likely fail to fully account for the uncertainty, leading to unsatisfactory inference; (ii) the use of smoothing splines implies a basis dimension equal to the number of observed data points, which can lead to substantial computational burden; in many applications, comparable fits can be achieved using lower-rank spline bases with far fewer basis functions (Wood, 2017, Chapter 5.2); (iii) because the mixed model representation of penalized splines is not exploited, the smoothing parameter must be selected separately from the remaining model components in a data-adaptive manner at each iteration. This further increases computational cost and limits the scalability of the method to large datasets.

Other estimation procedures for (2) have been considered in the literature. Elmi et al. (2011) represent the population curve using B-splines and evaluate the approximate marginal likelihood via adaptive Gaussian quadrature. Although treating the spline coefficients as fixed effects reduces the dimensionality of the integral, the computational cost of Gaussian quadra-

ture still increases rapidly with the dimension of the random effects. In addition, because smoothness is controlled solely through the number of knots rather than a penalty, this user choice becomes critical for obtaining an appropriate level of smoothness. More recent work (Arribas-Gil et al., 2013; De la Cruz et al., 2017; Márquez et al., 2023) considers additional semi-parametric approaches (e.g. a LASSO approach on a set of basis functions), but focuses on the case where the non-linear function does not depend on random effects, so that they can be integrated out explicitly without need for approximation. This greatly simplifies the method, but restricts its capabilities. In conclusion, a fully satisfactory algorithm for the model in (2) is not yet available, which has restricted the widespread use of SNMMs.

In this paper, we develop an estimation procedure for the SNMM based on a mixed-model representation of P-splines, which enables joint estimation of smoothness through variance components. The marginal likelihood is obtained via the Laplace approximation, with the required derivatives computed using automatic differentiation (AD), yielding efficient and accurate evaluation. The method is implemented using the R package TMB (Kristensen et al., 2016). The use of a unified likelihood, together with the availability of higher-order derivatives, allows inference on the population curve and the model parameters in a straightforward way directly from TMB.

The article is structured as follows. Section 2 describes our method in detail, shows the derivation of the marginal likelihood for the model through the Laplace approximation, and how AD is used to compute the necessary derivatives for estimation and inference; Section 3 presents simulated examples to study the performance of the method in comparison to the `assist` package; in Section 4, the method is illustrated using a dataset of height measurements of infants from birth to two years of age, and we show the use of a parametric bootstrap procedure to check the validity of the Laplace approximation in applications; a

discussion of the results and final remarks are included in Section 5.

## 2 Methods

### 2.1 Estimation

We start to describe the proposed estimation procedure for model (2) by expressing the population curve  $f$  as a penalized spline.

We explicitly show the dependence of the argument of  $f$  on the other parameters by writing  $f(\gamma(\phi_i; t_{ij}))$ ;  $\gamma$  is the x-axis transformation that  $f$  is subject to. We also use the notation  $u_i = \gamma(\phi_i; t)$  so that  $f$  is a function of  $u_i$ .

We consider  $f$  to be parametrized as

$$f(u) = \sum_{k=1}^K \theta_k c_k(u),$$

where  $c_k(\cdot)$  is the  $k$ -th basis function and  $\theta = (\theta_1, \dots, \theta_K)^\top$  are the corresponding spline coefficients. We can write

$$f(\gamma(\phi; t)) = \mathbf{X}(\phi, t)\theta \tag{3}$$

where the design matrix  $\mathbf{X}$  has elements  $X_{ij} = c_j(\gamma(\phi_i; t_{ij}))$ . Note that the design matrix in our model depends on the parameters  $\beta$  and  $b$  through  $\phi$ .

The level of smoothness is tuned by penalizing wiggleness, namely by a penalty of the form  $\lambda\theta^\top \mathbf{S}\theta$ , where  $\mathbf{S}$  is a penalty matrix (for example, based on finite differences of adjacent coefficients), and  $\lambda > 0$  is a smoothing parameter.

It is known that smoothing splines can be represented in a mixed model form (Kimeldorf and Wahba, 1970; Wang, 1998; Lin and Zhang, 1999, among others), in which components of the smooth in the null space of the penalty are treated as fixed effects, and the penalized

components as random. This allows smoothing parameters to be estimated via restricted maximum likelihood (REML) (Patterson and Thompson, 1971). Following Wood (2004), we can form the eigendecomposition  $\mathbf{S} = \mathbf{U}\mathbf{D}\mathbf{U}^\top$ , where  $\mathbf{U}$  is orthonormal and  $\mathbf{D}$  is diagonal (with eigenvalues arranged in decreasing order along the leading diagonal). We form  $\theta_u = \mathbf{U}^\top\theta$ . Since  $\mathbf{S}$  is generally rank-deficient, the last few elements on the leading diagonal of  $\mathbf{D}$  will be zero. Let  $\mathbf{D}^+$  denote the submatrix of  $\mathbf{D}$  containing only the nonzero elements on the leading diagonal, of dimension  $r \times r$ . Partition  $\theta_u$  so that  $\theta_u^\top = [\omega_u^\top, \theta_F^\top]$  and  $\theta_u^\top \mathbf{D} \theta_u = \omega_u^\top \mathbf{D}^+ \omega_u$ . Similarly, partition  $\mathbf{X}\mathbf{U}$  by letting  $\mathbf{X}_F$  contain the columns corresponding to zero entries on the diagonal of  $\mathbf{D}$ , and  $\mathbf{X}_u$  the ones corresponding to  $\mathbf{D}^+$ . By letting  $\omega = \sqrt{\mathbf{D}^+} \omega_u$ , the penalty  $\lambda \theta^\top \mathbf{S} \theta$  becomes  $\lambda \omega^\top \omega$ , which is equivalent to adding random effects  $\omega \sim N(0, \frac{1}{\lambda} \mathbf{I})$ . Defining  $\mathbf{X}_R = \mathbf{X}_u (\sqrt{\mathbf{D}^+})^{-1}$ , the matrix representation in (3) can be reparametrized as

$$f = \mathbf{X}_F \theta_F + \mathbf{X}_R \omega.$$

Now we go on to obtain the marginal likelihood for the model. Let  $\psi = (\mathbf{b}, \omega)$  be the complete vector of random effects, with  $\mathbf{b}_i$  associated with the subjects, and  $\omega$  coming from the representation of the smooth. Let  $\phi = (\theta_F, \beta, \Omega)$  be the vector of all fixed effects, which includes the unpenalized spline coefficients  $\theta_F$ , the fixed effects  $\beta$  and  $\Omega$  collecting the variance parameters, which determine  $\sigma$  and the random-effects covariance matrix  $G$ . Finally, let  $\tilde{G} = I_m \otimes G$  denote the block-diagonal covariance matrix of the random effects across all subjects. We can establish the conditional density of  $y$  given  $\psi$  as,

$$p(y|\psi) = (2\pi\sigma^2)^{-\frac{N}{2}} \exp \left\{ -\frac{1}{2\sigma^2} [y - \eta(\phi, f)]^2 \right\}$$

and the density of the random effects  $\psi$ ,

$$\begin{aligned} p(\psi) &= p(\mathbf{b})p(\omega) \\ &= (2\pi\sigma^2)^{-mq/2} |\tilde{G}|^{-1/2} (2\pi)^{-r/2} \lambda^{r/2} \exp \left( -\frac{1}{2\sigma^2} \mathbf{b}^\top \tilde{G}^{-1} \mathbf{b} - \frac{\lambda}{2} \|\omega\|^2 \right), \end{aligned}$$

which gives the joint density

$$\begin{aligned}
p(\mathbf{y}, \psi) &= p(\mathbf{y} \mid \psi) p(\psi) \\
&= (2\pi)^{-(N+mq+r)/2} (\sigma^2)^{-(N+mq)/2} |\tilde{\mathbf{G}}|^{-1/2} \lambda^{r/2} \\
&\quad \times \exp\left(-\frac{1}{2\sigma^2} \|\mathbf{y} - \eta(\phi, f)\|^2 - \frac{1}{2\sigma^2} \mathbf{b}^\top \tilde{\mathbf{G}}^{-1} \mathbf{b} - \frac{\lambda}{2} \|\omega\|^2\right).
\end{aligned} \tag{4}$$

The fixed parameters can be estimated by maximizing the marginal likelihood, obtained by integrating out the random effects from the joint density:

$$\begin{aligned}
L(\theta) &= \int p(\mathbf{y} \mid \psi) p(\psi) \, d\psi \\
&= (2\pi)^{-(N+mq+r)/2} (\sigma^2)^{-(N+mq)/2} |\tilde{\mathbf{G}}|^{-1/2} \lambda^{r/2} \int \exp\{g(\psi)\} \, d\psi,
\end{aligned} \tag{5}$$

with the exponent

$$g(\psi) = -\frac{1}{2\sigma^2} \|\mathbf{y} - \eta(\phi, f)\|^2 - \frac{1}{2\sigma^2} \mathbf{b}^\top \tilde{\mathbf{G}}^{-1} \mathbf{b} - \frac{\lambda}{2} \|\omega\|^2$$

from (4).

The  $(mq + r)$ -dimensional integral in (5) is generally intractable, because  $\eta$  depends nonlinearly on the random effects. The Laplace approximation is often used to approximate integrals in this setting (Ke and Wang, 2001; Wood, 2010), as it replaces the original integral with a closed-form expression based on a local Gaussian approximation to the integrand around its mode  $\hat{\psi} = \arg \max_{\psi} g(\psi)$ . This yields

$$g(\psi) \approx g(\hat{\psi}) - \frac{1}{2} (\psi - \hat{\psi})^\top \mathbf{H}(\hat{\psi}) (\psi - \hat{\psi}),$$

where  $\mathbf{H}(\hat{\psi}) = -\nabla^2 g(\hat{\psi})$  is the negative Hessian matrix of  $g$  evaluated at the mode. It follows that the Laplace approximate marginal log-likelihood is

$$\begin{aligned}
l(\theta) &= N \log \sqrt{2\pi} - (N + mq) \log(\sigma) - \frac{1}{2} \log |\tilde{\mathbf{G}}| + \frac{r}{2} \lambda \\
&\quad - \frac{1}{2} \log |\mathbf{H}(\theta)| + g\{\hat{\psi}(\theta), \theta\},
\end{aligned} \tag{6}$$

where we have expressed explicitly the dependence of  $\mathbf{H}$ ,  $\hat{\psi}$ , and  $g$  on  $\theta$ .

Computation of the Laplace approximation involves two main steps: (1) obtaining the mode by maximizing  $g(\psi)$ , and (2) evaluating the Hessian of  $g$  at that mode. Both steps require first and second-order derivatives of  $g$  with respect to  $\psi$ . Given the complexity of the model, deriving these expressions by hand would be tedious, error-prone, and their final form would still depend on the specific functional choice of  $\eta(\cdot)$ , and the basis functions used. To avoid these difficulties, AD was employed to compute the required derivatives of  $g$ . AD computes numerical derivatives accurate to machine precision by systematically applying the chain rule to every elementary operation in a program (Griewank and Walther, 2008; Skaug and Fournier, 2006). Our implementation used the R package Template Model Builder, TMB (Kristensen et al., 2016), which relies on CppAD for forward and reverse mode AD via operator overloading (Bell, 2005).

The estimation in TMB proceeds hierarchically. For starting values of the fixed parameters,  $\theta$ , TMB first locates the conditional mode of the random effects,  $\hat{\psi}(\theta) = \arg \max_{\psi} g(\psi; \theta)$ , using Newton optimization. At the optimum, the Hessian with respect to the random effects is computed for the Laplace approximation to the marginal likelihood. TMB then computes the gradient of this Laplace-approximated objective with respect to  $\theta$ . This allows the use of any gradient-based optimization routine to find the maximum of the marginal likelihood with respect to the fixed parameters: in our implementation we used the `nlminb` function in R, which employs a quasi-Newton trust-region method from the PORT routines (Gay, 1990). The final estimates of the fixed effects correspond to the maximizer of the marginal likelihood, while the estimates of the random effects are given by their modes evaluated at the optimal values of the fixed parameters.

## 2.2 Inference

At convergence of the optimization problem, the covariance matrix of the estimated fixed effects  $\text{Var}(\hat{\theta})$  can be obtained from the inverse of the observed Hessian of the (approximated) marginal log-likelihood (6),

$$\text{Var}(\hat{\theta}) = \left[ -\nabla_{\theta}^2 l(\hat{\theta}) \right]^{-1}.$$

The delta method is then used by TMB to obtain a first-order approximation to the covariance matrix of any differentiable function of the fixed parameters  $\phi(\hat{\theta})$ :

$$\text{Var}(\phi(\hat{\theta})) \approx \mathbf{J}_{\phi} \text{Var}(\hat{\theta}) \mathbf{J}_{\phi}^{\top}, \quad \mathbf{J}_{\phi} = \left. \frac{\partial \phi(\theta)}{\partial \theta^{\top}} \right|_{\theta=\hat{\theta}}.$$

In order to obtain inferences for the population and subject-level spline curves, the method has to be extended to functions of both fixed and random effects. However, since the estimate of the random effects  $\hat{\psi}(\theta)$  depends on  $\theta$ , its variance has to take into account the uncertainty in the estimation of  $\theta$ , which requires further derivation.

We are interested in the covariance matrix of the estimation errors on the random and fixed effects, which is given by

$$\text{Var} \begin{pmatrix} \hat{\psi} - \psi \\ \hat{\theta} - \theta \end{pmatrix} \approx \begin{pmatrix} \mathbf{H}^{-1} & \mathbf{0} \\ \mathbf{0} & \mathbf{0} \end{pmatrix} + \mathbf{J} \text{Var}(\hat{\theta}) \mathbf{J}^{\top},$$

where  $\mathbf{J}$  is the Jacobian of  $[\hat{\psi}(\theta), \theta]^{\top}$  with respect to  $\theta$  (the derivation of this formula can be found in the book version of [Kristensen \(2016\)](#), Appendix 16.3). With this, we can use the delta method to express the variance of the estimation error on a general function of fixed and random effects  $f(\theta, \psi)$ :

$$\text{Var}(f(\hat{\psi}, \hat{\theta}) - f(\psi, \theta)) \approx \nabla f \text{Var} \begin{pmatrix} \hat{\psi} - \psi \\ \hat{\theta} - \theta \end{pmatrix} \nabla f^{\top}.$$

Zheng and Cadigan (2021) discuss in detail the interpretation of this variance, which they denote *prediction variance*. When using prediction variance, inferences about the random effects will be appropriate only for the specific values of the random effects of the observed data. This procedure, however, does not describe the variability of the estimator  $\hat{\psi}$  caused by the repeated sampling of  $\psi$ .

To construct a confidence band, we first extract from TMB the estimated values of the target function evaluated on a grid of points, denoted by  $\hat{f}$ , together with the corresponding covariance matrix of the estimation errors,  $\hat{V}$ . A pointwise Wald-type confidence band with nominal level  $(1 - \alpha)100\%$  is then given by  $\hat{f} \pm z_{1-\alpha/2} \sqrt{\text{diag}(\hat{V})}$ , where  $z_{1-\alpha/2}$  denotes the  $\alpha/2$  quantile of the standard normal distribution. Confidence bands constructed in this manner attain coverage close to the nominal level on average over the domain of the function. In contrast, obtaining simultaneous coverage of the entire function with probability  $(1 - \alpha)100\%$  requires replacing the normal critical value with one obtained via simulation. Further methodological details are provided in (Sørensen et al., 2023, Section 1.1).

## 2.3 Further considerations

### 2.3.1 Knot selection

Because  $f$  is a function of the latent values  $\gamma(\phi; t)$ , the appropriate locations for knots are not directly observable. Moreover, knot placement determines the structure of the penalty matrix  $\mathbf{S}$ , which must be decomposed into its null space and range space to express the spline coefficients as fixed and random effects. Allowing the knot locations to depend on the random effects would cause the matrix  $\mathbf{S}$  and its eigendecomposition to depend on the model parameters. Incorporating such procedure within AD would be infeasible. For these reasons, we would prefer fixing the knot locations throughout estimation.

We consider two approaches to do this, depending on the nature of  $\gamma$ . The first applies when  $\gamma$  is known to take values in a finite and fixed interval, as in the first simulation study presented in Section 3. In this case, the range of  $\gamma$  is known, and the knots can therefore be fixed on a given interval which safely covers the support of the function.

In the second case, we consider functions whose domains are not bounded a priori. To retain a fixed set of knots, we modify  $\gamma$  so that its codomain is predictable over the observed range of  $t$  and over plausible values of the random effects. Specifically, the lower and upper bounds of  $\gamma$  are defined using the observed values of  $t$  and values of  $\phi$  within  $\pm 3$  standard deviations of their current estimated variances. To preserve compatibility with AD, these bounds are expressed as smooth functions of the model parameters.

For example, if  $\gamma(\phi; t) = t - b_3$  (as in the second simulation of Section 3), the bounds can be defined as

$$\min \gamma = \min(t) - 3\sigma_{b_3}, \quad \max \gamma = \max(t) + 3\sigma_{b_3},$$

so that both depend smoothly on the estimated variance of  $b_3$ . The transformed variable is then standardized as

$$\gamma^*(\phi, t, \Omega) = \frac{\gamma(\phi; t) - \min \gamma(\Omega)}{\max \gamma(\Omega) - \min \gamma(\Omega)}, \quad \gamma^*(\phi; t) \in [0, 1].$$

By construction,  $\gamma^*$  takes values in  $[0, 1]$  over the relevant domain of the variables, allowing knots to be placed at fixed locations in  $[0, 1]$ . Note that  $\gamma^*$  now depends explicitly on the variance parameters  $\Omega$  through  $\sigma_{b_3}$ . This construction yields a fixed penalty matrix while allowing the transformation to adapt smoothly to changes in the variance parameters, preserving differentiability.

### 2.3.2 Starting values

Estimation of the approximated marginal likelihood is performed using a gradient-based optimization procedure and therefore requires starting values for all model parameters; however, finding suitable values is often nontrivial.

Following [Elmi et al. \(2011\)](#), we suggest adopting a two-step strategy. First, starting values for the spline coefficients can be obtained by fitting a generalized additive model to the raw data. Second, treating this fitted curve as known, a nonlinear mixed-effects model can be fitted using R package `nlme` ([Pinheiro and Bates, 2000](#)) to obtain starting values for the fixed effects and random-effects variance components. Although this procedure does not involve joint estimation, it is computationally efficient and has shown to provide sensible starting values in our experience.

## 3 Simulation studies

First, we compare our estimation and inference procedure (labeled “snmmTMB”) with the R package `assist`. We consider the same simulated data setup reported in [Ke and Wang \(2001\)](#). Specifically, we generate data from the model

$$y_{ij} = 1 + b_{1i} + \exp(b_{2i}) \sin 2\pi \left( \frac{i}{n} - \frac{\exp(b_{3i})}{1 + \exp(b_{3i})} \right) + \varepsilon_{ij}, \quad i = 0, \dots, n, \quad j = 1, \dots, m,$$

with errors  $\varepsilon_{ij} \sim \mathcal{N}(0, \sigma^2)$  and random effects vector  $\mathbf{b}_i = (b_{1i}, b_{2i}, b_{3i})^\top \sim \mathcal{N}(\mathbf{0}, \sigma^2 \mathbf{D})$ . In this formulation,  $b_{1i}$  represents a subject vertical shift,  $b_{2i}$  is a curve scaling factor, and  $b_{3i}$  introduces a subject phase shift.

We consider all possible combinations of parameter values on the grid: (1)  $\sigma^2 \in \{1, 0.4\}$ ; (2)  $m \in \{10, 20\}$ ; (3)  $n \in \{10, 20\}$ ; (4) low-variance  $\mathbf{D} = \text{diag}(0.25, 0.16, 0.04)$ , or high-variance  $\mathbf{D} = \text{diag}(1, 0.25, 0.16)$ ; for a total of 16 data settings. Each setting is simulated 300 times

to obtain the results of Figures 1 and 2.

For `smmmTMB`, we use a cubic spline basis with penalty based on second-order finite differences. The knots are distributed uniformly in  $[-1, 1]$ , as we see that the phase shift function  $\gamma(b, t_{ij}) = t_{ij} - \frac{\exp(b_{3i})}{1 + \exp(b_{3i})}$ , takes values in this interval, independently of the values of  $b_{3i}$ . The `assist` method specifications are chosen in line with the description of the simulation in Ke and Wang (2001); we need to provide a model space for  $f$ , which is chosen as the periodic functions  $\text{span}\{\sin(2\pi x), \cos(2\pi x)\}$ . Note that the model is thus given information about the periodicity of the underlying population curve.

Both methods produce a confidence band around the estimated population curve, and in Figure 1 we compare: (i) the simultaneous coverage of the whole population curve and (ii) the average width of the confidence band. We can see that the `assist` method obtains low coverage in the settings with high variance parameters, for all sample sizes, despite being provided information on the underlying function being periodic through the model space definition; in contrast, coverage for `smmmTMB` is more stable around the nominal value for all settings. In terms of confidence band width, `smmmTMB` consistently achieves a narrower band, which tends to get smaller with larger sample size; this value is larger and more unstable in the case of `assist`. In terms of computational cost, the average runtimes across the different simulation settings ranged between 5.67 and 39.2 seconds for `smmmTMB`, compared to a range of 7.60 and 170.0 seconds for `assist`. While runtimes vary across settings, `smmmTMB` was consistently faster and exhibited less variability. A more detailed investigation of computational time for increasing sample size is presented in online Appendix A.

Finally, our method also allows the production of confidence bands for subject-level curves, which combine the uncertainty on the population curve and the subject random effects.

Figure 2 shows that the coverage is optimal in this task as well. As expected, the confidence intervals are much larger in the settings with fewer observations per subject, as there is more uncertainty on the subject curve.

As a second simulation example, we consider a bell-shaped curve, generated from the model

$$y_{ij} = 1 + b_{1i} + \exp\left(-\frac{1}{2}(t_{ij} - b_{2i})^2\right) + \varepsilon_{ij}, \quad i = 0, \dots, n, \quad j = 1, \dots, m,$$

with parameter values: (1)  $\sigma^2 \in \{0.2, 0.4\}$ ; (2)  $m \in \{10, 20\}$ ; (3)  $n \in \{10, 20\}$ ; and fixed  $\mathbf{D} = \text{diag}(2, 2)$ , for a total of 8 data settings. The parameters  $b_{1i}$  and  $b_{2i}$  represent a subject vertical and horizontal shift respectively. In this case, the knots are selected with the knot scaling procedure described in Section 2.3.1. Specifically, the knots are fixed in the interval  $[0, 1]$ , and the internal function  $\gamma$  is scaled accordingly to take values in that range. `assist` is applied by calculating the reproducing kernel for cubic splines.

Figure 3 shows the comparison. Once again, `smmmTMB` achieves coverage close to the nominal level, while `assist` exhibits substantially lower coverage in all settings despite producing, on average, wider confidence bands. Based on our experience with `assist`, this behavior appears to be related to difficulties in selecting an appropriate level of smoothness, with a tendency toward undersmoothing that leads to undercoverage.

## 4 Application

We illustrate our approach using a longitudinal subsample of the Social Medical Survey of Children Attending Child Health Clinics (SMOCC), which followed Dutch children born in 1988–1989 with repeated measurements of height during the first two years of life (Herngreen et al., 1994). The original study investigated early childhood growth in relation to socioeconomic status; however, socioeconomic information is not included in the publically

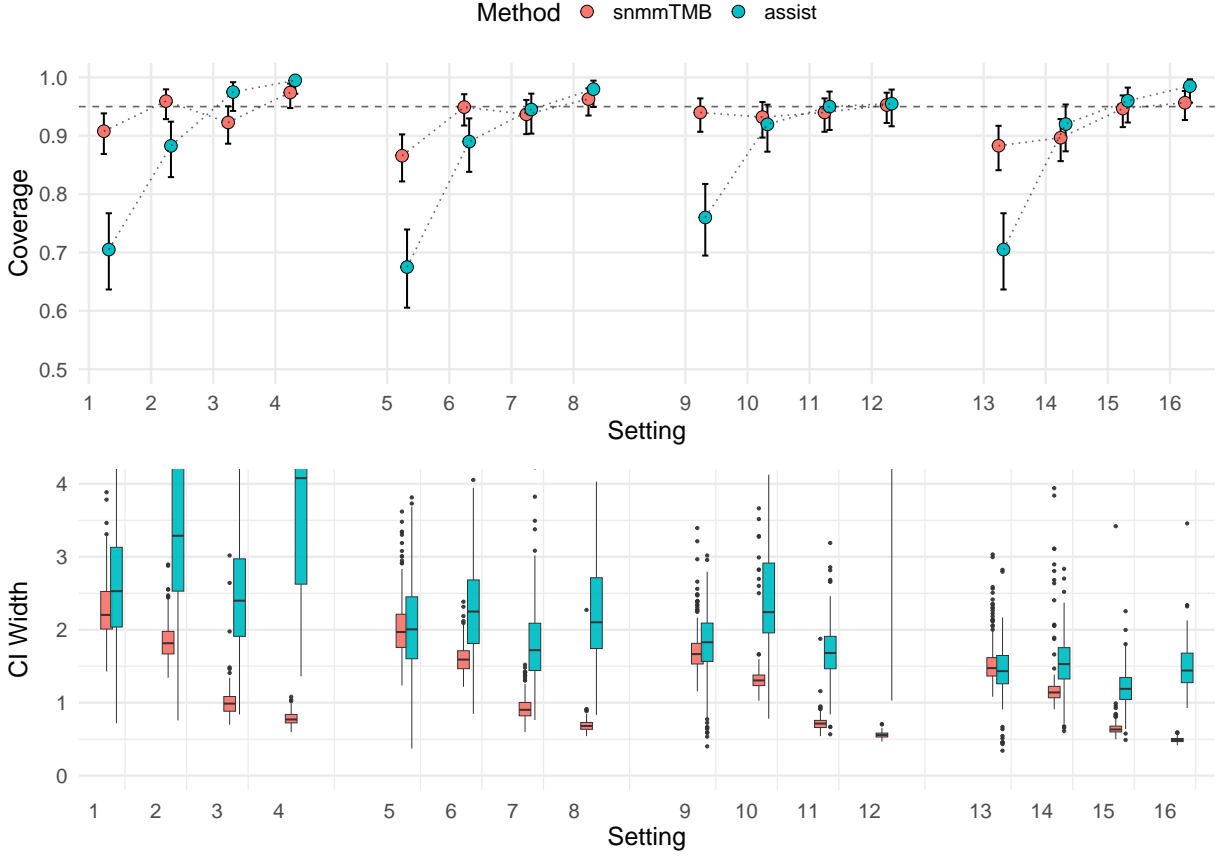


Figure 1: *Results of the sine curve simulation on the population curve.* The first four settings correspond to  $(n, m, \sigma, D)$  equal to  $(10, 10, 1, \text{high})$ ,  $(10, 10, 1, \text{low})$ ,  $(10, 10, 0.4, \text{high})$ , and  $(10, 10, 0.4, \text{low})$ . The remaining groups of 4 follow the same order but with sample sizes  $(10, 20)$ ,  $(20, 10)$ , and  $(20, 20)$ . The top panel displays the average simultaneous coverage of the population curve across 300 replications; bars indicate binomial confidence intervals for the coverage probability. The bottom panel shows boxplots of the average confidence-band width; for visual clarity, some results from `assist` fall outside the plotting range.

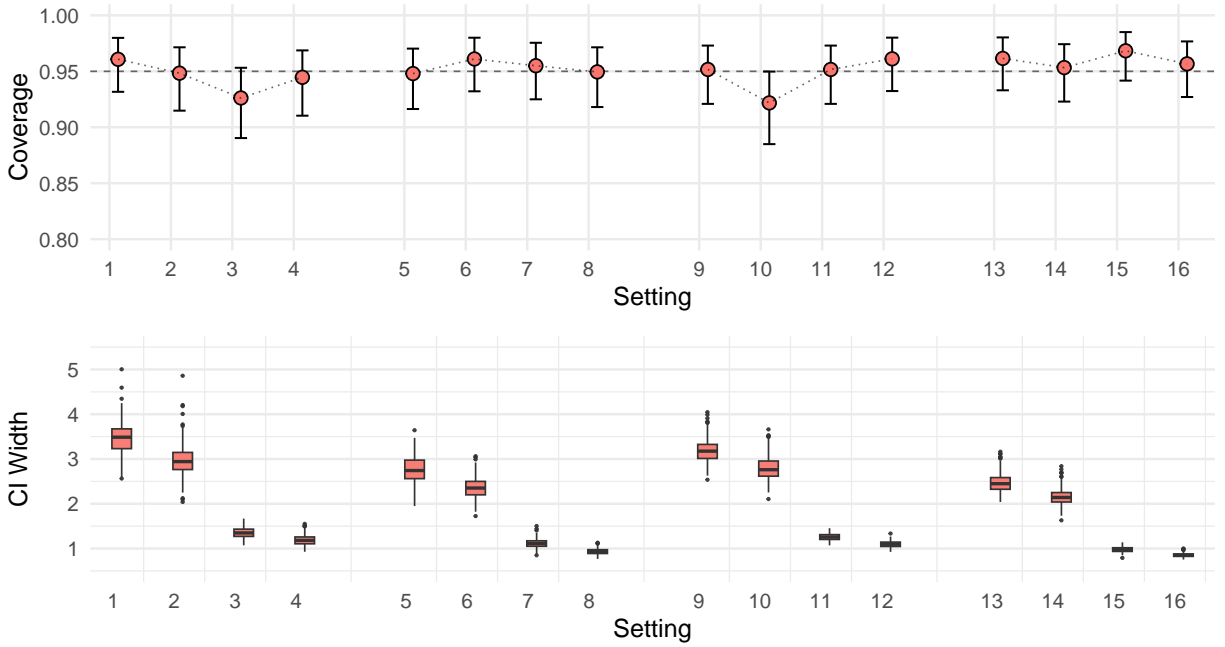


Figure 2: *Results of the sine curve simulation on the subject curves.* The parameter settings follow those of Figure 1. The top panel displays the average simultaneous coverage of the subject curves across 300 replications; bars indicate binomial confidence intervals for the coverage probability. The bottom panel shows boxplots of the average confidence-band width.

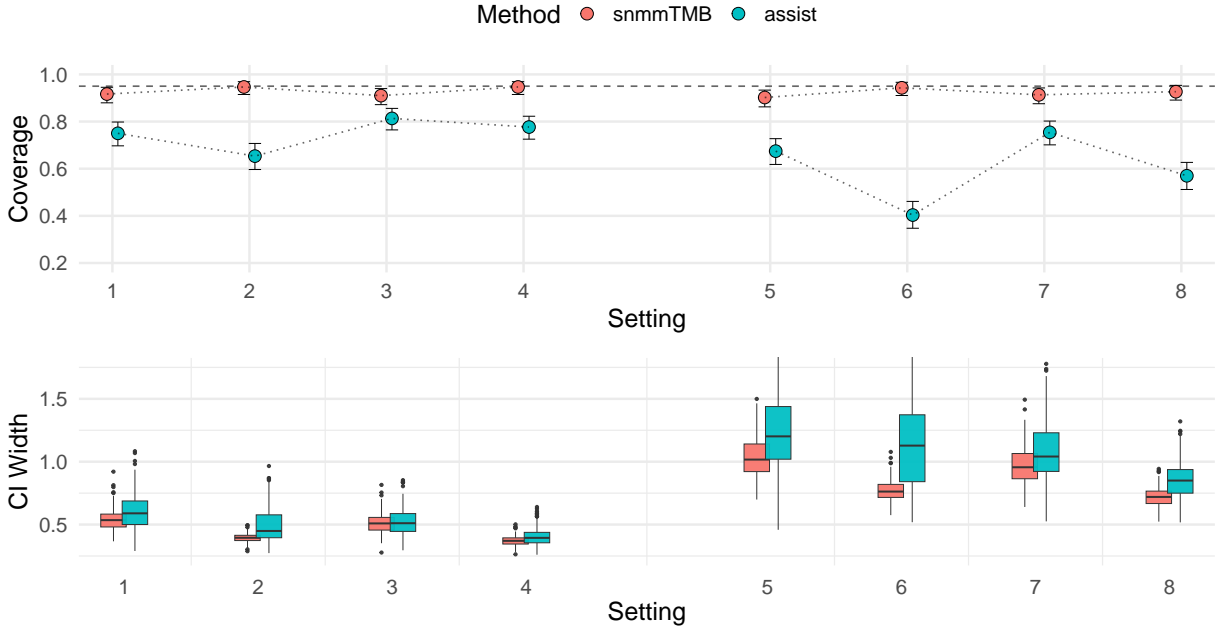


Figure 3: *Results of the bell curve simulation on the population curve.* The first four settings correspond to  $(n, m, \sigma)$  equal to  $(10, 10, 0.2)$ ,  $(20, 10, 0.2)$ ,  $(10, 20, 0.2)$ , and  $(20, 20, 0.2)$ . The remaining groups of 4 follow the same order but with error variance 0.4. The top panel displays the average simultaneous coverage of the population curve across 300 replications; bars indicate binomial confidence intervals for the coverage probability. The bottom panel shows boxplots of the average confidence-band width.

available subsample of the data considered here. The aim of this analysis is to demonstrate how longitudinal growth data of this type can be modeled within the SNMM framework. Specifically, we use the model to estimate a smooth population curve of height growth by age with covariate effects on the intercept, scale, and shift parameters, while allowing for subject-specific deviations through random effects. In addition, we describe a parametric bootstrap procedure that can be used in applied settings to assess the adequacy of the Laplace approximation underlying the likelihood-based estimation.

The data contains 200 subjects, with each subject measured between 6 and 12 times (1942 total observations). We include two covariates: sex (coded as 0-female/1-male), and gestational age (GA), measured as deviation in weeks from the average pregnancy length of 40 weeks. Several candidate model specifications were considered, and the fixed-effects structure was chosen using the marginal Akaike information criterion (AIC) (Vaida and Blanchard, 2005). A broader discussion of model selection, including considerations for random effects, is provided in Section 5.

The following model was fit to the data:

$$\begin{aligned} \text{hgt}_{ij} &= \beta_0 + \beta_1 \text{sex}_i + b_{1i} + \exp(\beta_2 \text{sex}_i) f(\text{age}_{ij} + \beta_3 \text{GA} + b_{3i}) + \epsilon_{ij}, \\ \mathbf{b}_i &\sim N(\mathbf{0}, \mathbf{D}), \quad \epsilon_{ij} \sim N(0, \sigma^2 \mathbf{I}), \end{aligned}$$

with a diagonal covariance matrix  $\mathbf{D} = \text{diag}(\sigma_{b_1}^2, \sigma_{b_2}^2)$ . The response variable (height in centimeters), is modeled with a penalized cubic B-spline basis with 11 internal knots, subject to sum-to-zero constraint. The fixed coefficients represent:  $\beta_0$ , the baseline height level for female subjects (sex = 0);  $\beta_1$ , the intercept difference between males and females;  $\beta_2$ , a sex-specific scaling of the population growth trajectory, which accounts for differences in growth rate;  $\beta_3$ , the shift along the age axis associated with gestational age, so that differences in weeks of prematurity or post-term birth translate into horizontal shifts of the growth curve.

The random effect  $b_{1i}$  accounts for subject-specific deviations in overall height level, whereas  $b_{3i}$  allows individual-specific timing shifts of the growth trajectory relative to the population curve.

The estimated curve for some representative subjects is shown, with simultaneous confidence bands and observed data, in Figure 4. The estimated trajectory exhibits the well-known pattern of rapid increase during the first six months (de Onis, 2006), followed by a more gradual growth over the remainder of the observation period. Overall, between-subject variability appears limited, with individual curves closely tracking the population trend.

Parameter estimates are given in Table 1. The intercept effect of sex  $\beta_1$  indicates that male subjects are, on average, approximately 1.8 cm taller at birth than female subjects. The sex-specific scaling of the growth trajectory  $\beta_2$  is not statistically significant, indicating no clear evidence of differences in growth rate between male and female subjects in the model. The gestational-age shift  $\beta_3$  on the time axis is close to 1, suggesting that being born one week premature or overdue translates almost one-to-one into the corresponding shift in measured height at birth.

For the Wald confidence intervals reported in Table 1 to be reliable, the marginal log-likelihood must be adequately approximated by a quadratic function around its maximum. A parametric bootstrap can be used to examine this assumption and to evaluate potential bias in both parameter estimates and their associated standard errors (Sørensen et al., 2023, Section 4.2). In this procedure, multiple datasets are generated from the fitted model by resampling the subject random effects and noise, and the model is re-estimated for each simulated dataset. We note that the random effects associated with the spline coefficients are only considered a computational approach to achieve smoothness, thus we generate bootstrap samples using the fitted parameter values rather than drawing new smooth functions

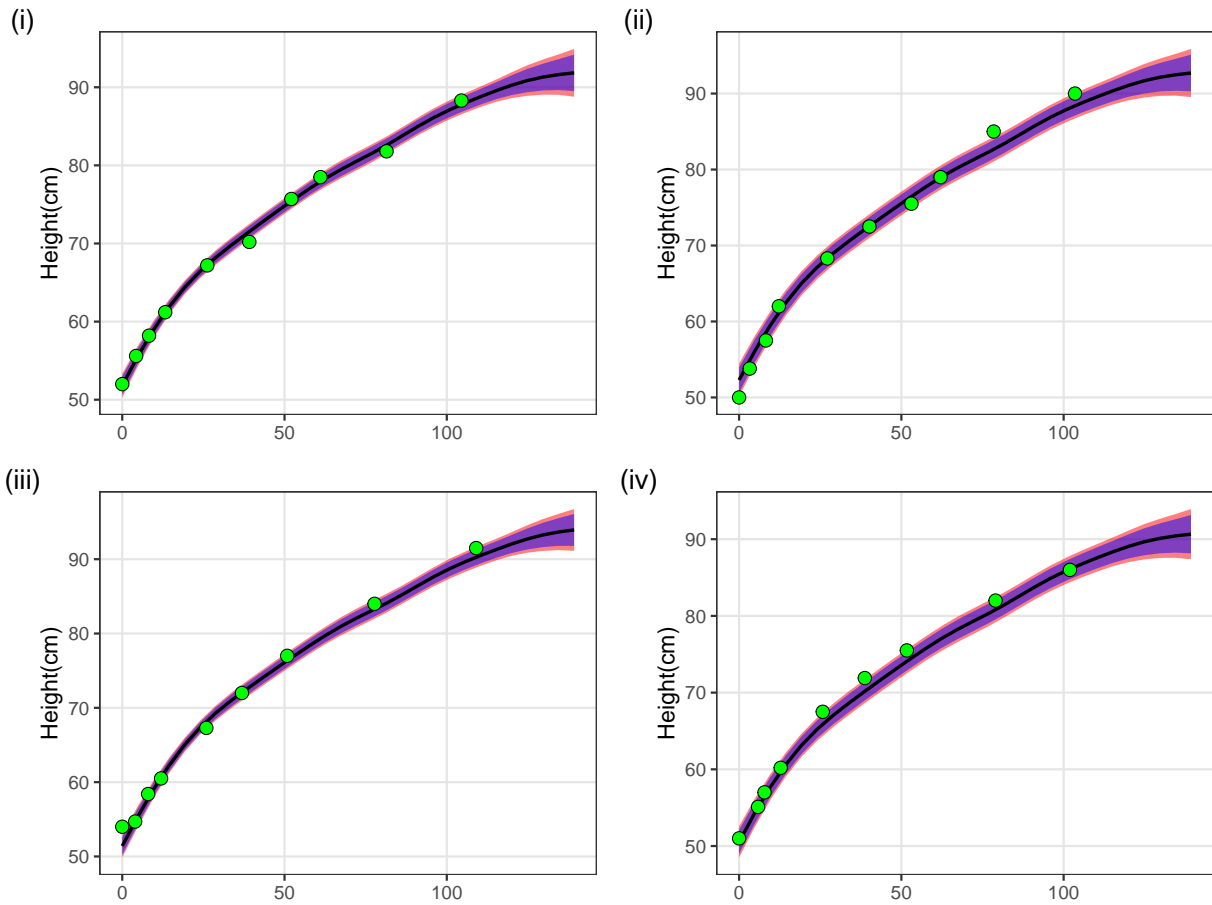


Figure 4: *Height observations and model-based fits for four individuals.* Green points denote observed height measurements. The solid black line shows the estimated mean growth trajectory, with the blue and red shaded areas representing pointwise and simultaneous confidence bands respectively. Sex and gestational age are (i) Female, 40 weeks; (ii) Male, 36 weeks; (iii) Female, 41 weeks; (iv) Male, 38 weeks.

Variable	Estimate (95% Wald CI)
Intercept ( $\beta_0$ )	68.2 (67.6 – 68.7)
Sex (male) intercept ( $\beta_1$ )	1.80 (0.92 – 2.68)
Sex (male) scale ( $\beta_2$ )	0.00 (-0.01 – 0.01)
Gestational age shift ( $\beta_3$ )	1.00 (0.73 – 1.27)
$\sigma_{b_1}$	2.86 (2.56 – 3.17)
$\sigma_{b_2}$	3.28 (2.89 – 3.68)
$\sigma$	1.05 (1.01 – 1.09)

Table 1: Parameter estimates for the SMOCC data model.

for each replication.

If the quadratic approximation is adequate, the variability of the bootstrap estimates should be consistent with the standard errors derived from the asymptotic covariance matrix, implying satisfactory coverage of Wald-type intervals. Figure 5 summarizes the results by plotting the original parameter estimates against their bootstrap averages, and the empirical standard deviation of the bootstrap estimates against the corresponding average asymptotic standard errors. Overall, the point estimates are well tracked by their bootstrap means, and the asymptotic standard errors appear to provide an adequate approximation of the sampling variability. The coefficients showing the largest deviation are the intercepts,  $\beta_0$  and  $\beta_1$ . If more accurate inference for these parameters were required, bootstrap-based inference could be used as an alternative to Wald-type intervals.

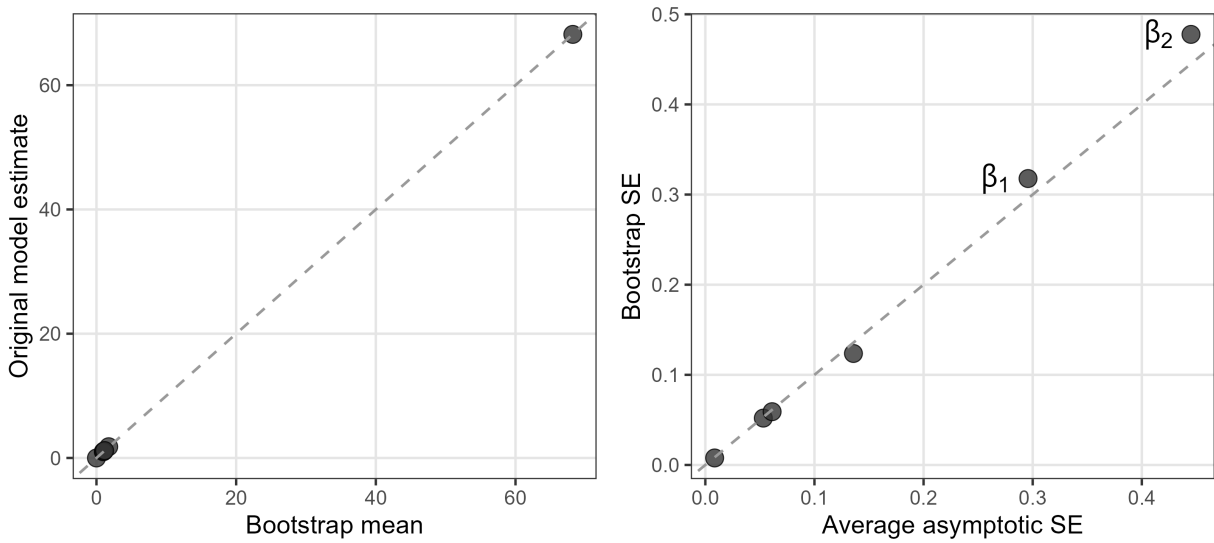


Figure 5: *Parametric bootstrap assessment of bias and standard errors.* The left panel shows the original parameter estimates against their bootstrap averages. The right panel shows the empirical standard deviation of the bootstrap estimates versus the average asymptotic standard errors. Results from 200 simulations. The standard error for  $\beta_1$  and  $\beta_2$  deviate most from their bootstrap average and are labeled.

## 5 Discussion

We have presented a procedure for estimation and inference for the semiparametric non-linear mixed-effects model of [Ke and Wang \(2001\)](#). We introduce two main adaptations: (i) the population trajectory is represented through a penalized spline expressed in mixed-model form, which allows us to estimate the smoothing parameter as a variance component, without requiring additional smoothness selection procedures; (ii) the marginal likelihood is evaluated through the Laplace approximation, with the required derivatives obtained by AD. Across simulations the procedure obtained accurate point estimates and improved coverage of the population curve, with narrower confidence bands, when compared to the original estimation approach. Application to infant height data between birth and two years produced population trajectories and parameter estimates consistent with the established pattern of early-life growth, illustrating the practical applicability of the proposed framework.

Model selection was performed on fixed-effects using marginal AIC, while keeping the random-effects structure fixed. Selecting random effects would instead require using a conditional AIC ([Vaida and Blanchard, 2005](#)), but the standard form does not account for uncertainty in estimated variance parameters and therefore tends to favor inclusion of any random effects with positive variance ([Greven and Kneib, 2010](#)). An adjusted conditional AIC that incorporates variance and smoothing-parameter uncertainty has been proposed for general smooth models by [Wood et al. \(2016\)](#); extending this approach to the SNMM framework represents a useful direction for future work.

Identifiability is an important aspect to consider when fitting an SNMM. Different combinations of spline components and model parameters can yield equivalent likelihoods, for example when shifts or scaling of the population curve are confounded with intercept or scale parameters. Although these issues are highly case-specific, they can often be addressed

by imposing appropriate constraints on the spline, such as a sum-to-zero constraint to ensure identifiability of an intercept term, or by restricting scale parameters to be positive. Theoretical discussions of identifiability of similar models can be found in [Kneip and Gasser \(1988\)](#) and [Lindstrom \(1995\)](#).

We used a B-spline basis to represent the population curve. Other spline bases could be considered as well, provided that their evaluation and derivatives can be implemented in a differentiable manner in C++, to ensure compatibility with AD.

In many applications, it is desirable to enforce shape constraints on the population curve (e.g. monotonicity, convexity) based on prior knowledge of the underlying process, as unconstrained models might give implausible results. These constraints are often imposed by reparametrizing the spline coefficients ([Pya and Wood, 2014](#)); however, this approach is hard to apply in our framework, as the coefficients are represented as mixed effects to enforce smoothness. A more accessible alternative is to encourage shape properties through penalties on the spline derivatives. This strategy is discussed further in online Appendix B.

The implementation in TMB is naturally flexible and can accommodate several extensions to the model specification that were not explored here. These include relaxing the Gaussian error assumption to allow non-Gaussian responses through appropriate link functions and adopting alternative random-effects covariance structures. Incorporating multiple smooth components or interaction terms through additional penalized splines could also be possible, although in such settings careful attention to identifiability and appropriate constraints becomes even more important.

## 6 Disclosure statement

The authors declare no conflict of interest.

## 7 Data Availability Statement

The code for reproducing the simulated and real examples and the SMOCC dataset used as example in the article are available on GitHub at <https://github.com/matteodales/snmmTMB>.

## References

- Altman, N. and J. Villarreal (2004, September). Self-modelling regression for longitudinal data with time-invariant covariates. *Canadian Journal of Statistics* 32(3), 251–268.
- Arribas-Gil, A., K. Bertin, C. Meza, and V. Rivoirard (2013, February). LASSO-type estimators for semiparametric nonlinear mixed-effects models estimation. *Statistics and Computing* 24(3), 443–460.
- Bell, B. M. (2005). *CppAD: a package for C++ algorithmic differentiation*. Computational Infrastructure for Operations Research (COIN-OR).
- Cole, T. J., M. D. C. Donaldson, and Y. Ben-Shlomo (2010, December). SITAR—a useful instrument for growth curve analysis. *International Journal of Epidemiology* 39(6), 1558–1566.
- Coull, B. A. and J. Staudenmayer (2004). Self-Modeling Regression for Multivariate Curve Data. *Statistica Sinica* 14(3), 695–711.
- De la Cruz, R., C. Fuentes, C. Meza, and A. Arribas-Gil (2017, February). Predicting pregnancy outcomes using longitudinal information: a penalized splines mixed-effects model approach. *Statistics in Medicine* 36(13), 2120–2134.

- de Onis, M. (2006, April). WHO Child Growth Standards based on length/height, weight and age. *Acta Paediatrica* 95(S450), 76–85.
- Elmi, A., S. J. Ratcliffe, S. Parry, and W. Guo (2011, January). A B-Spline Based Semiparametric Nonlinear Mixed Effects Model. *Journal of Computational and Graphical Statistics* 20(2), 492–509.
- Gay, D. M. (1990). Usage summary for selected optimization routines. Technical Report Computing Science Technical Report No. 153, AT&T Bell Laboratories, Murray Hill, NJ.
- Greven, S. and T. Kneib (2010). On the behaviour of marginal and conditional AIC in linear mixed models. *Biometrika* 97(4), 773–789.
- Griewank, A. and A. Walther (2008, January). *Evaluating Derivatives: Principles and Techniques of Algorithmic Differentiation, Second Edition*. Society for Industrial and Applied Mathematics.
- Herngreen, W., S. van Buuren, J. van Wieringen, J. Reerink, S. Verloove-Vanhorick, and J. Ruys (1994). Growth in length and weight from birth to 2 years of a representative sample of Netherlands children (born in 1988–89) related to socioeconomic status and other background characteristics. *Annals of Human Biology* 21(5), 449–463.
- Ke, C. and Y. Wang (2001, December). Semiparametric Nonlinear Mixed-Effects Models and Their Applications. *Journal of the American Statistical Association* 96(456), 1272–1298.
- Kimeldorf, G. S. and G. Wahba (1970). A Correspondence Between Bayesian Estimation on Stochastic Processes and Smoothing by Splines. *The Annals of Mathematical Statistics* 41(2), 495–502.
- Kneip, A. and T. Gasser (1988, March). Convergence and Consistency Results for Self-Modeling Nonlinear Regression. *The Annals of Statistics* 16(1), 82–112.

- Kristensen, K. (2016). TMB Documentation: Comprehensive Documentation of C++ Functions and Classes (API). [Accessed 31-10-2025].
- Kristensen, K., A. Nielsen, C. W. Berg, H. Skaug, and B. M. Bell (2016). TMB: Automatic Differentiation and Laplace Approximation. *Journal of Statistical Software* 70(5), 1–21.
- Lawton, W. H., E. A. Sylvestre, and M. S. Maggio (1972). Self modeling nonlinear regression. *Technometrics* 14(3), 513–532.
- Lin, X. and D. Zhang (1999, July). Inference in Generalized Additive Mixed Models by Using Smoothing Splines. *Journal of the Royal Statistical Society Series B: Statistical Methodology* 61(2), 381–400.
- Lindstrom, M. J. (1995, September). Self-modelling with random shift and scale parameters and a free-knot spline shape function. *Statistics in Medicine* 14(18), 2009–2021.
- Lindstrom, M. J. and D. M. Bates (1990, September). Nonlinear Mixed Effects Models for Repeated Measures Data. *Biometrics* 46(3), 673.
- Márquez, M., C. Meza, D.-J. Lee, and R. De la Cruz (2023, September). Classification of longitudinal profiles using semi-parametric nonlinear mixed models with P-Splines and the SAEM algorithm. *Statistics in Medicine* 42(27), 4952–4971.
- Patterson, H. D. and R. Thompson (1971). Recovery of inter-block information when block sizes are unequal. *Biometrika* 58(3), 545–554.
- Pinheiro, J. C. and D. M. Bates (2000). *Mixed-Effects Models in S and S-PLUS*. New York: Springer-Verlag.
- Pya, N. and S. N. Wood (2014, February). Shape constrained additive models. *Statistics and Computing* 25(3), 543–559.

- Skaug, H. J. and D. A. Fournier (2006, November). Automatic approximation of the marginal likelihood in non-Gaussian hierarchical models. *Computational Statistics & Data Analysis* 51(2), 699–709.
- Sørensen, Ø., A. M. Fjell, and K. B. Walhovd (2023, June). Longitudinal Modeling of Age-Dependent Latent Traits with Generalized Additive Latent and Mixed Models. *Psychometrika* 88(2), 456–486.
- Vaida, F. and S. Blanchard (2005). Conditional Akaike Information for Mixed-Effects Models. *Biometrika* 92(2), 351–370.
- Wang, Y. (1998, January). Mixed Effects Smoothing Spline Analysis of Variance. *Journal of the Royal Statistical Society Series B: Statistical Methodology* 60(1), 159–174.
- Wang, Y. and C. Ke (2004, February). assist: A Suite of R Functions Implementing Spline Smoothing Techniques.
- Wood, S. N. (2004, September). Stable and Efficient Multiple Smoothing Parameter Estimation for Generalized Additive Models. *Journal of the American Statistical Association* 99(467), 673–686.
- Wood, S. N. (2010, September). Fast Stable Restricted Maximum Likelihood and Marginal Likelihood Estimation of Semiparametric Generalized Linear Models. *Journal of the Royal Statistical Society Series B: Statistical Methodology* 73(1), 3–36.
- Wood, S. N. (2017, May). *Generalized Additive Models: An Introduction with R*. Chapman and Hall/CRC.
- Wood, S. N., N. Pya, and B. Säfken (2016, October). Smoothing Parameter and Model Selection for General Smooth Models. *Journal of the American Statistical Association* 111(516), 1548–1563.

Zheng, N. and N. Cadigan (2021, August). Frequentist delta-variance approximations with mixed-effects models and TMB. *Computational Statistics & Data Analysis* 160, 107227.

# Appendices for “A Semiparametric Nonlinear Mixed Effects Model with Penalized Splines Using Automatic Differentiation”

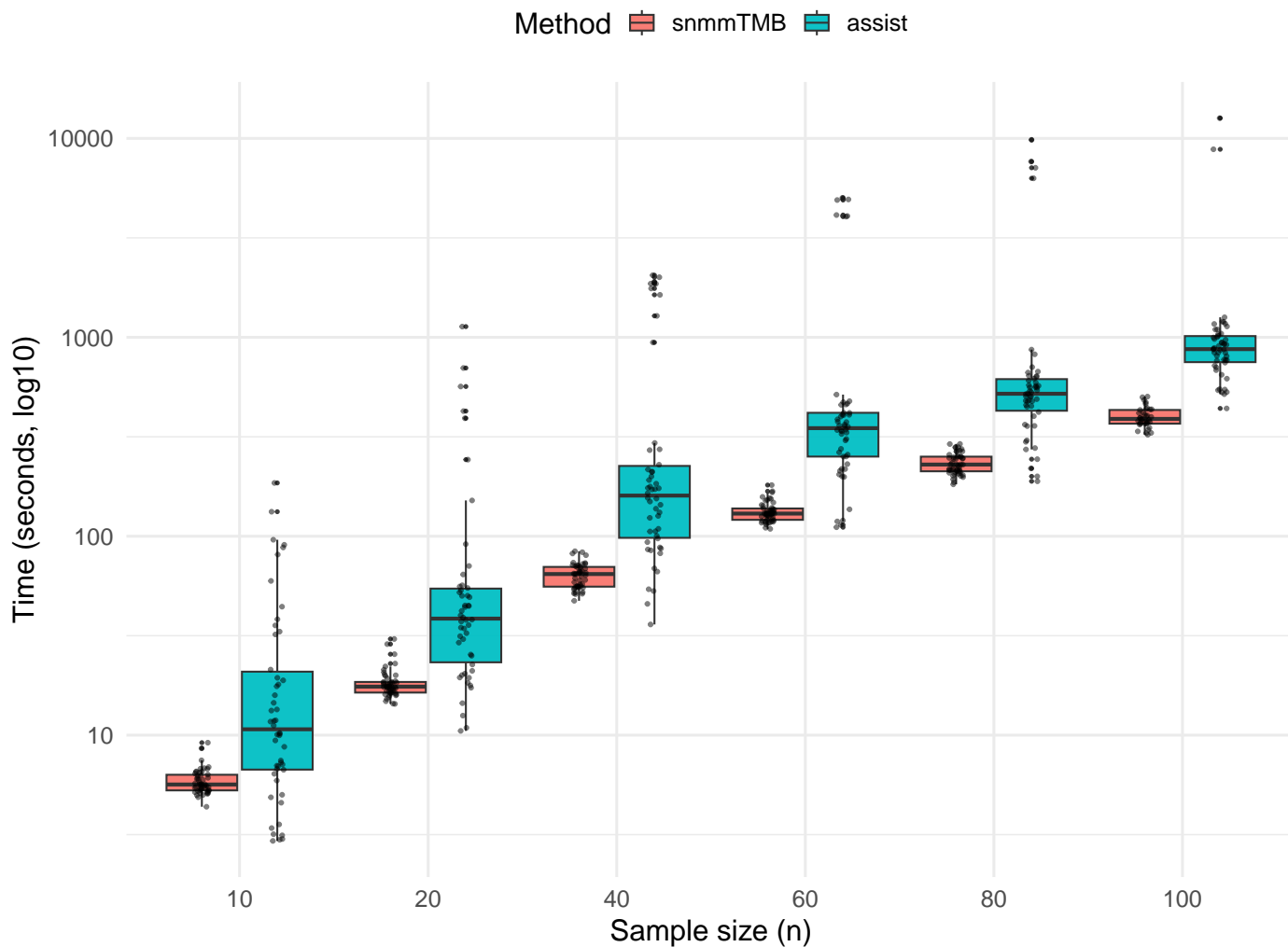
## A Computational time

Supplementary Figure 1 shows boxplots of runtimes for `snmmTMB` and `assist` as the number of subjects  $n$  increases. Across all sample sizes, `assist` has substantially more variable computational times, with many iterations resulting in very long runs. In contrast, `snmmTMB` displays much more stable performance and is consistently faster on average.

The `assist` method relies on an iterative algorithm that alternates between estimating the smooth population curve and fitting a nonlinear mixed-effects model to update fixed and random effects. Because this procedure does not optimize a unique cost function, convergence is not guaranteed and the number of iterations can vary widely, leading to occasional extremely slow runs.

## B Monotonicity

As mentioned in the Discussion, it is often desirable to impose shape constraints such as monotonicity when prior knowledge about the underlying population trajectory is available. In our framework, direct constraints on spline coefficients are difficult to impose because smoothness is enforced by representing penalized components as random effects within a mixed-model formulation. Instead, we suggest a penalty-based approach that promotes monotonicity while preserving the mixed-model structure and remaining compatible with automatic differentiation. Similar asymmetric penalties have been proposed in Eilers (2005); Bollaerts et al. (2006); Hofner et al. (2014).



Supplementary Figure 1: *Computational time comparison.* Boxplots of runtime for snmmTMB and assist for increasing numbers of subjects  $n = 10, 20, 40, 60, 80, 100$ . Each setting is repeated for 100 iterations. The simulation setting corresponds to the first simulation scenario in Section 3, with  $m = 10$ ,  $\sigma = 1$ , and  $\mathbf{D} = \text{diag}(1, 0.25, 0.16)$ . The time axis is shown on a logarithmic scale.

Through the TMB implementation, additional penalty terms can easily be incorporated directly into the negative log-likelihood without altering the underlying model specification. Moreover, derivatives of B-splines can be evaluated efficiently using standard recursion formulas.

Let the population smooth be represented using a B-spline basis as

$$f(x) = \sum_{k=1}^K \theta_k B_k(x),$$

where  $B_k(\cdot)$  are B-spline basis functions and  $\theta_k$  are the corresponding coefficients. Under the mixed-model representation, the full vector of spline coefficients  $\boldsymbol{\theta}$  can be reconstructed from the fixed and random components at each iteration of the optimization. The derivative of a B-spline of degree  $p$  can be expressed as a linear combination of two B-splines of degree  $p-1$ , which allows the derivative of the smooth to be written as

$$f'(x) = \sum_{k=1}^K \theta_k B'_k(x),$$

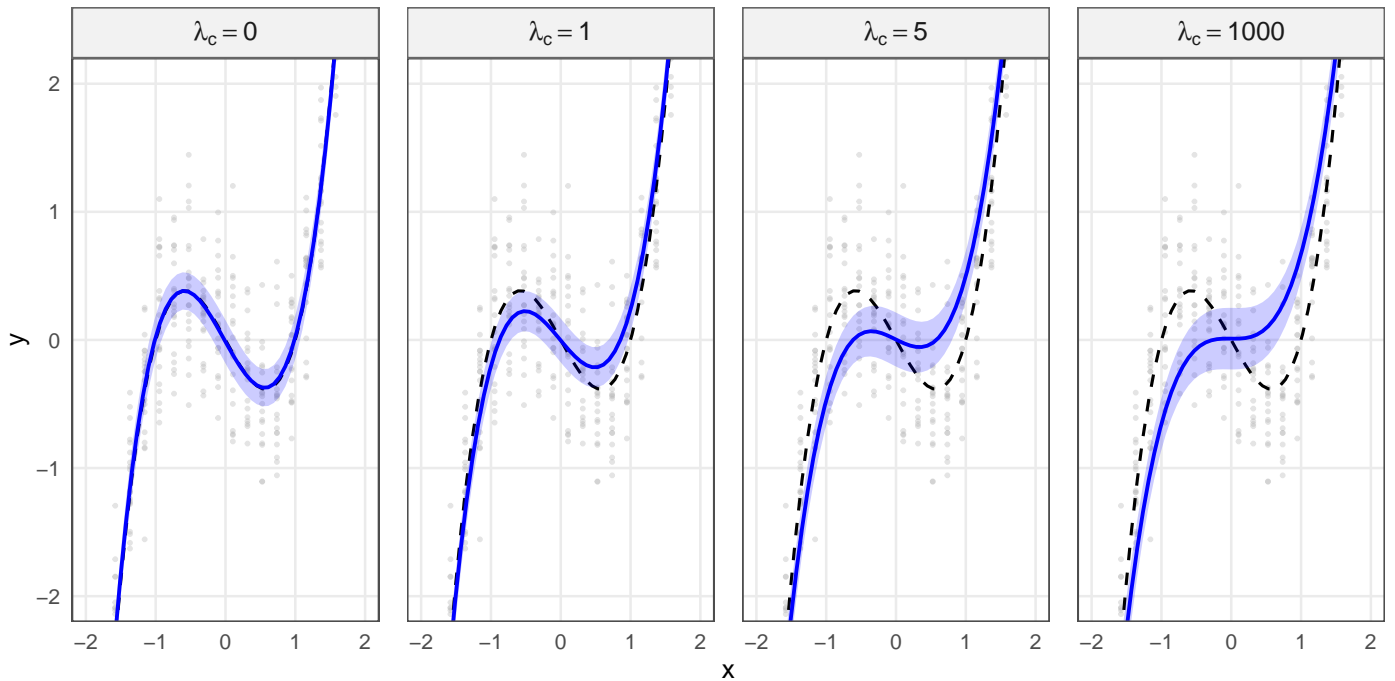
and evaluated at arbitrary points with a very small computational cost. Specifically, we obtain  $B'_k$  from function `splineDesign` from R package `splines`.

To promote monotonicity, we can then evaluate  $f'(x)$  on a dense grid of points  $\{x_i\}_{i=1}^M$  spanning the domain of interest and introduce an asymmetric penalty that penalizes negative derivatives while leaving positive derivatives unaffected. Specifically, we define the penalty

$$\lambda_c \sum_{i=1}^M [\min(f'(x_i), 0)]^2,$$

where  $\lambda_c > 0$  controls the strength of the constraint. Since the function  $\min(f'(x), 0)$  is not differentiable, a smooth approximation is required for compatibility with automatic differentiation. We can replace it with the smooth approximation

$$\min(f'(x), 0) \approx \frac{1}{2} \left( \sqrt{f'(x)^2 + \varepsilon} - f'(x) \right),$$



Supplementary Figure 2: *Effect of the monotonicity penalty on spline estimation.* Simulated data are generated from the function  $y = x^3 - x$ . Points represent the observed data, the dashed black line denotes the true function, and the solid blue line shows the estimated population curve with an increasing value of the monotonicity penalty  $\lambda_c = 0, 1, 5, 1000$ , and its associated simultaneous confidence band. As  $\lambda_c$  increases, the fitted curve becomes progressively less decreasing.

where  $\varepsilon$  is a small positive constant. This approximation is everywhere differentiable and numerically stable, and for sufficiently large values of  $\lambda_c$ , the estimated curve is effectively constrained to be monotone increasing.

To illustrate the effect of the penalty, we present a simulation example in Supplementary Figure 2, which shows fitted curves obtained under increasing values of  $\lambda_c$ . The data are generated on the interval  $[-2, 2]$  from the function  $y = x^3 - x$ , which is not monotone. Accordingly, fitting the spline without the monotonicity penalty (Panel A) yields a correctly non-monotone estimate. As the penalty weight increases, the estimated population curve becomes progressively less decreasing.

We note that similar penalties could be put on the second derivative of the curve to induce convexity.

## References

- Bollaerts, Kaatje, Paul H. C. Eilers, and Iven van Mechelen (Nov. 2006). “Simple and multiple P-splines regression with shape constraints”. In: *British Journal of Mathematical and Statistical Psychology* 59(2), pp. 451–469. ISSN: 2044-8317. DOI: [10.1348/000711005x84293](https://doi.org/10.1348/000711005x84293). URL: <http://dx.doi.org/10.1348/000711005X84293>.
- Eilers, Paul H. C. (May 2005). “Unimodal smoothing”. In: *Journal of Chemometrics* 19(5–7), pp. 317–328. ISSN: 1099-128X. DOI: [10.1002/cem.935](https://doi.org/10.1002/cem.935). URL: <http://dx.doi.org/10.1002/cem.935>.
- Hofner, Benjamin, Thomas Kneib, and Torsten Hothorn (Oct. 2014). “A unified framework of constrained regression”. In: *Statistics and Computing* 26(1–2), pp. 1–14. ISSN: 1573-1375. DOI: [10.1007/s11222-014-9520-y](https://doi.org/10.1007/s11222-014-9520-y). URL: <http://dx.doi.org/10.1007/s11222-014-9520-y>.